Tau Neutrino Detection

Edmond Ng

December 2019

1 Introduction/Background

The goal of this project was to explore the performance of a neutrino detector in identifying tau neutrinos. This project builds upon previous work done by Meng [1]. High energy tau neutrinos produce two cascades of light, one from the hadronic shower produced by the CC interaction and the other by the lepton decay. If the separation between the two is sufficient, by analyzing the distribution photon arrival time, a double peak signature my be visible.

2 Main Simulation Setup

The simulation for generating high energy neutrinos in a detector was built upon the one used by Meng [1]. For details of the simulation refer to [1]. To briefly summarize, the simulation consists of a 150 m cubic detector fill with seawater and contains 9 strings with 12 sensors evenly spaced. To generate neutrino events, since GEANT4 cannot handle neutrino interaction with matter, the lepton and hadronic shower produced in a CC interaction are simulated independently. For instance, to simulate a 100 TeV electron neutrino a 50 TeV electron and 50 TeV hadronic shower are simulated. The particles are injected at the event vertex located at (-10 m, -20 m, -62.5 m) [1] with a velocity oriented in the +z direction (See Figure 1). The simulation tracks the photons that hit a sensor, and records the position and time. For tau events, the simulation also returns the decay time, which is a new addition to the code.

3 Optical Properties of Seawater in GEANT4 Simulations

The optical properties of seawater at the P-ONE site was explored in [2] and are summarized in Table 1. These parameters were included in the GEANT4 simulation. For details of the implementation see [1].

An exploration into the scattering and absorption of light in the GEANT4 simulation was done to ensure that the simulations adequately reflect the optical properties at the P-ONE site. This was done by creating a spherical detector in GEANT4 (see Figure 2) filled with 200 sensors either 54.5 m or 88.1 m away from the center. Light was emitted isotropically from the center, and the arrival time of the photons was recorded. The distances were chosen to match the distance from POCAM2 to sDOM1 and POCAM2 to sDOM3 respectively (see

[1] This is different from Meng's simulation which had the event vertex at (-20 m, -10 m, -62.5 m)

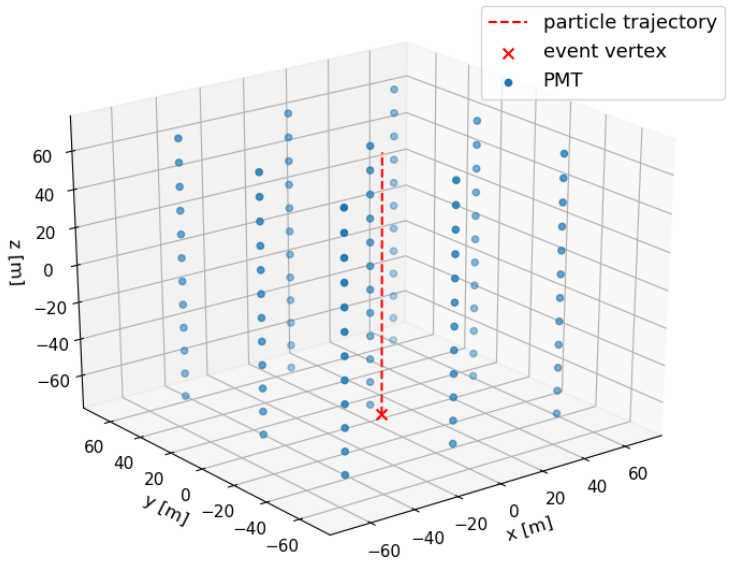

Figure 1: Detector setup in GEANT4 . The detector is a 150x150x150 m cube filled with seawater, containing 9 strings with 12 sensors on each string. The particle is injected at the event vertex (-10 m, -20 m, -62.5 m) marked with a red 'x', and the dashed red line represents the particle trajectory.

Wavelength (nm)	Photon Energy (eV)	λ_{abs} (m)	λ_{sct} (m)
465 (blue)	2.666	55.0	32.3
405 (violet)	3.061	35.0	19.0
365 (uv)	3.396	30.5	10.6

Table 1: The optical properties of water, including the absorption length λ_{abs} and scattering length λ_{sct}, at the Cascadia basin for different wavelengths of light. Results from Mar-19 STRAW data by Matthew Man in [2]

[3]). The light from a POCAM is not emitted instantaneously but rather it is a gaussian with a FWHM of 10 ns [3], thus the time residuals from the simulation was convoluted with the beam shape to obtain the correct shape for the time residuals. The result from the simulation is shown in Figure 3.

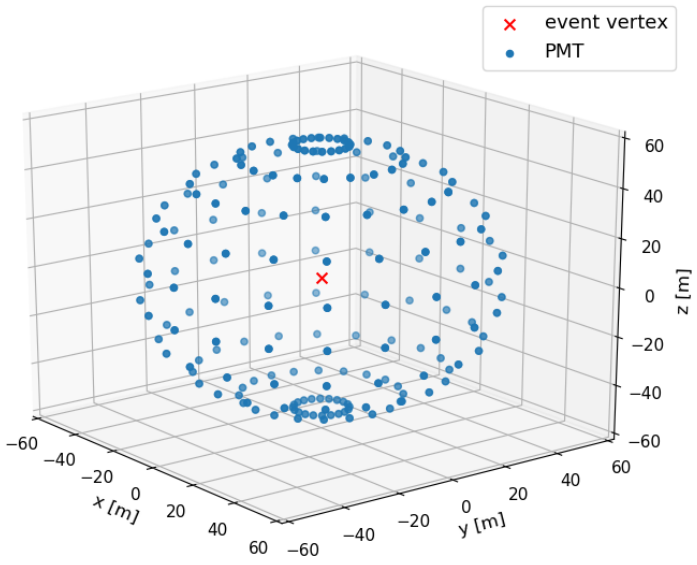

Figure 2: Spherical detector setup in GEANT4 . The detector is a sphere filled with seawater, containing 200 sensors 54.4 m from the center. The photons are injected at the event vertex located at the center marked with a red 'x', and given a random trajectory.

The resulting simulation is compared with Mar-19 STRAW data in Figure 4 and Figure 5.

In general the time residuals from the GEANT4 simulation and data agree near the peak, but not for the tails. The tails from the data have a steeper drop compared to the GEANT4 simulation. This indicates that there is more scattering in the simulation compared to the data. Through this comparison we see that the propagation of photons through seawater in GEANT4 is sufficiently close to the optical properties at the Cascadia basin for the purposes of this project.

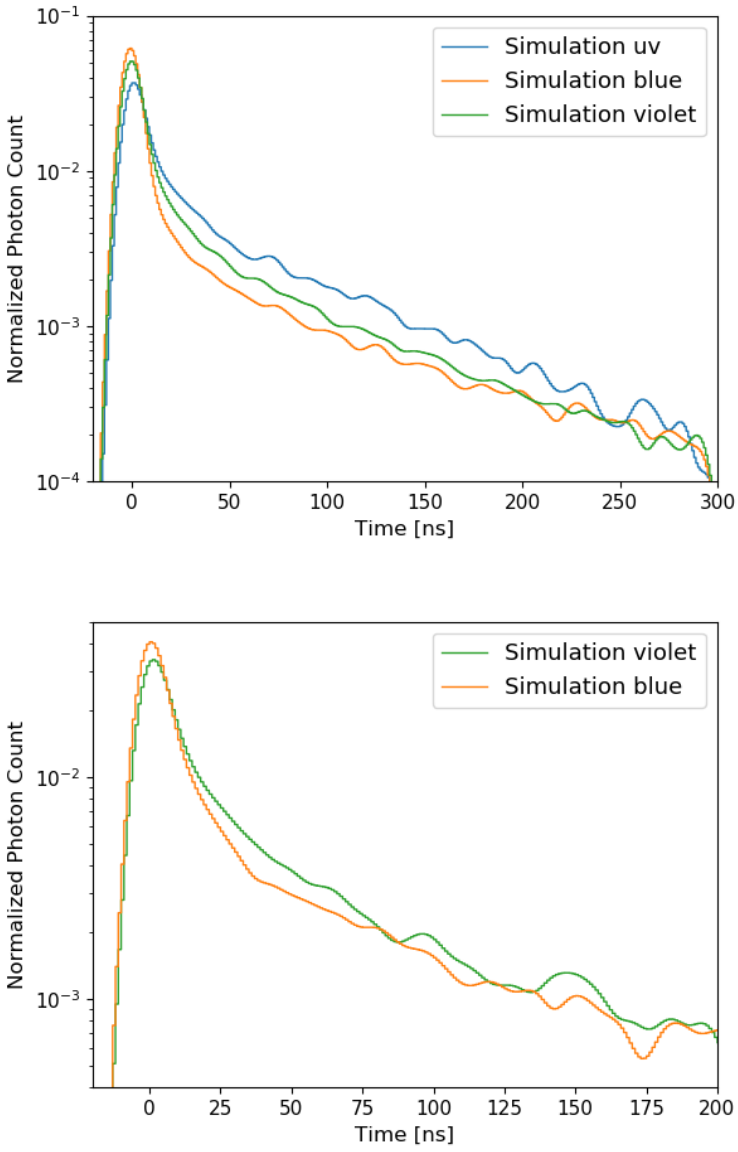

Figure 3: A plot of the distribution of photon arrival time from the GEANT4 simulation with the bin size fixed at 1 ns convoluted with the pulse shape of a POCAM, which is a gaussian with a FWHM of 10 ns. Top: Sensors are 54.5 m from the light source. Bottom: Sensors are 88.1 m from the light source.

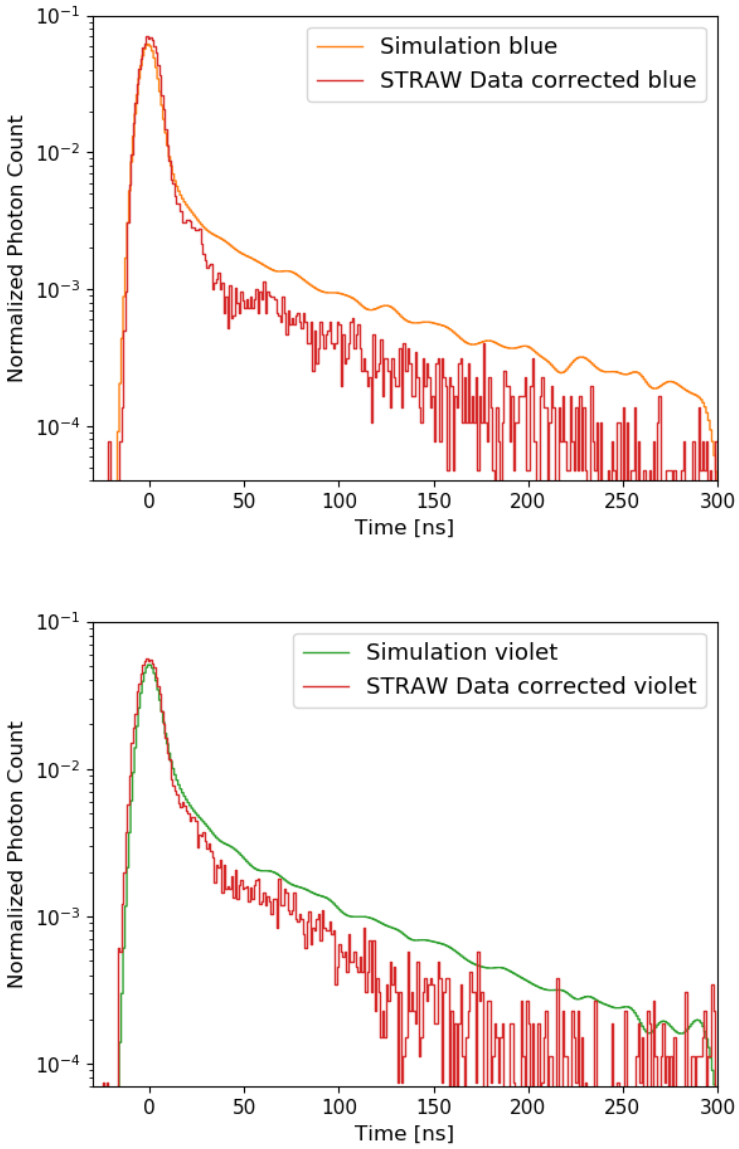

Figure 4: Time residuals, for the arrival time of photons in the GEANT4 simulation compared to Mar-19 STRAW data. Results for a sensor distance at 54.4m, for blue and violet light.

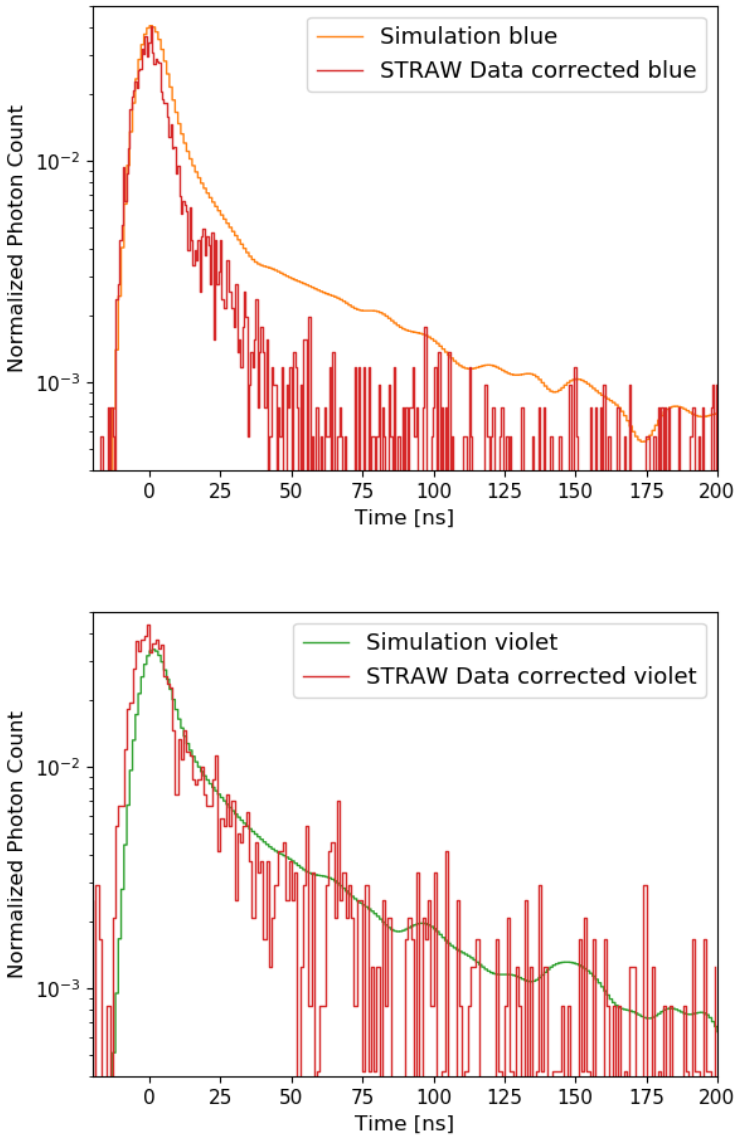

Figure 5: Time residuals, for the arrival time of photons in the GEANT4 simulation compared to Mar-19 STRAW data. Results for a sensor distance at 88.1 m, for blue and violet light.

4 Simulation

For this project 100 tau neutrino and e neutrino events at 20, 100 and 200 TeV, with the energy split evenly between the lepton and the hadronic shower.

4.1 Decay Time

The decay time of the 100 tau events generated at each energy was recorded and the distribution at 10 and 100 TeV are shown for in Figure 6. Comparison between the expected mean decay time and the mean decay time for the simulations are presented in Table 2.

Energy (TeV)	Expected Mean Decay Time (ns)	Simulation Mean Decay Time (ns)
10	1.63	1.94 $\pm$ 0.26
50	8.16	8.90 $\pm$ 0.73
100	16.32	18.09 $\pm$ 1.43

Table 2: The expected decay time of a tau lepton at a specific energy compared with the mean tau decay time in the GEANT4 simulations.

4.2 Hits Distribution

The number of photons that hits for each event was recorded. For the electron and hadronic shower, the number of hits roughly scales linearly with the energy and there is little variation in the distribution of hits. The average number of hits at each energy is presented in Table 3 and the distribution of the number of hits at 50 TeV for the electron and hadronic shower is shown in Figure 7. In contrast, tau events have a wide range of hits based on the decay mode [4] as shown in Figure 8. For our analysis We will not consider tau events that decay into muons.

Energy (TeV)	Hits e-	Hits Hadronic Shower
10	34939 $\pm$ 562	29448 $\pm$ 945
50	178205 $\pm$ 2015	153827 $\pm$ 3745
100	358549 $\pm$ 3115	315051 $\pm$ 6644

Table 3: The average number of photons that hit a PMT for e- events and the hadronic shower at different energies.

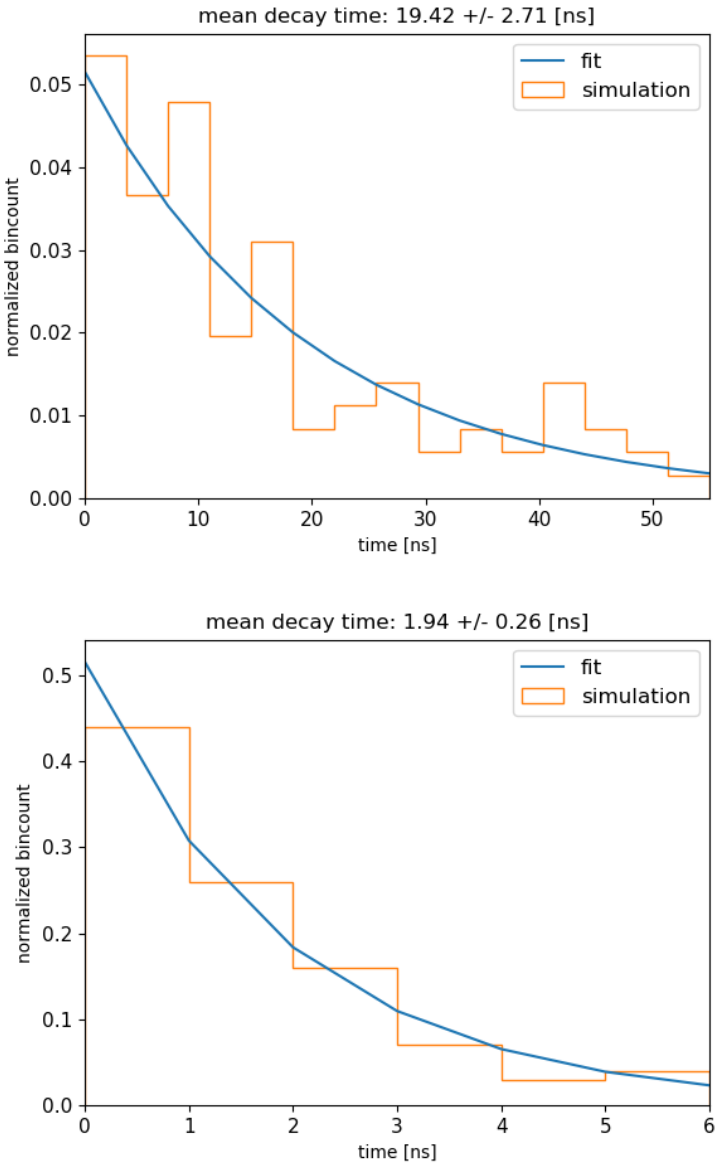

Figure 6: A plot of the distribution of tau decay times in the 100 events generated at 100 TeV (top) and 10 TeV (bottom). The mean decay time is found by fitting the distribution with an exponential.

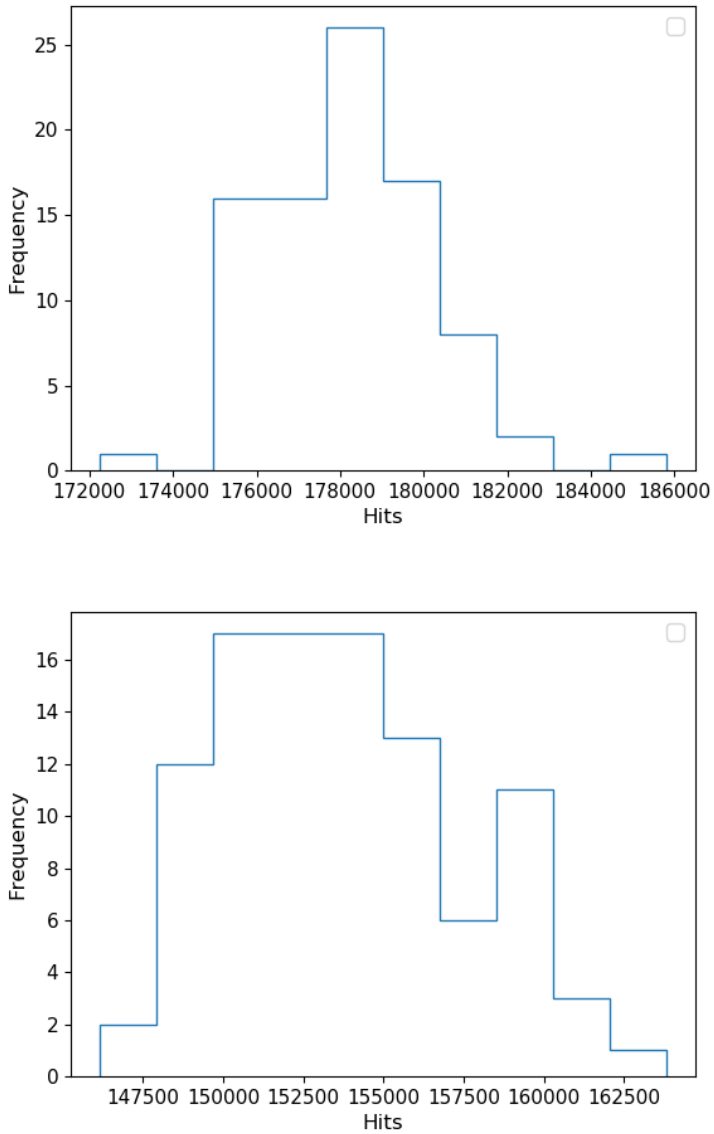

Figure 7: Plot of the distribution of the number of photons that hit a sensor for the simulations at 50 TeV. Top: Hit distribution for the e-. Bottom: Hit distribution for the hadronic shower.

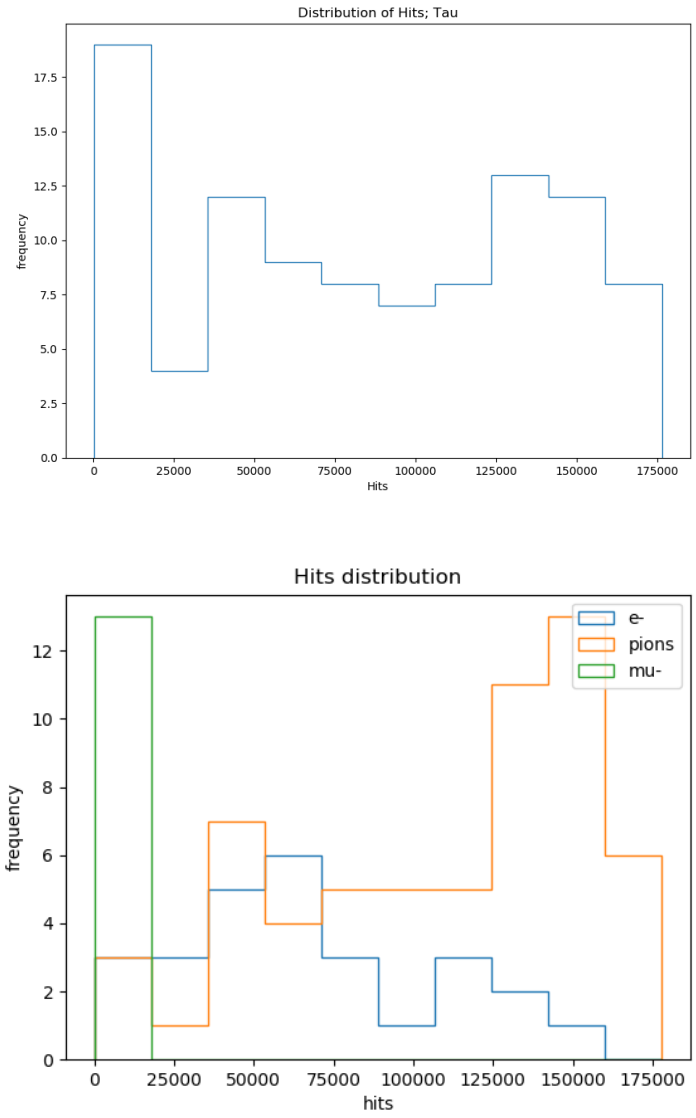

Figure 8: Plot of the distribution of the number of photons that hit a sensor for the tau lepton simulations at 50 TeV. Top: Hit distribution. Bottom: Hit distribution breakdown into the different tau decay modes.

5 Results

5.1 Photon Arrival Time and Depth

The arrival time of photons at different depths was explored. This was done with a separate simulation altered slightly, with the event vertex was at (-20 m, -62.5 m, -10 m) and with the particle moving in the +y direction (see Figure 9). A plot of the photon arrival time at different depths for one event is shown in Figure 10.

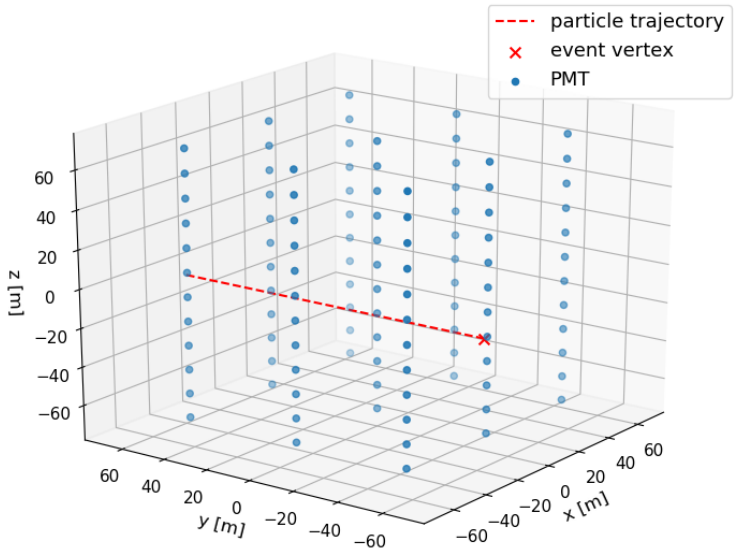

Figure 9: Detector setup in GEANT4 for the simulation exploring the hit time vs depth !!!. The detector is a 150x150x150 m cube filled with seawater, containing 9 strings with 12 sensors on each string. The particle is injected at the event vertex (-20 m, -62.5 m, -10 m) marked with a red 'x', and the dashed red line represents the particle trajectory.

For a single light shower propagating in the +y direction, the light should hit the sensors and produce a hyperbolic shape as seen in Figure 10. The idea for this analysis that was for tau neutrinos, the two showers would be separated so that there could be two overlapping hyperbolas, providing an complimentary method for identifying tau neutrinos. However this was not the case, there is not enough separation spatially between the hadronic shower and the shower from the tau decay for any significant difference to be noticed between tau and electron neutrino events.

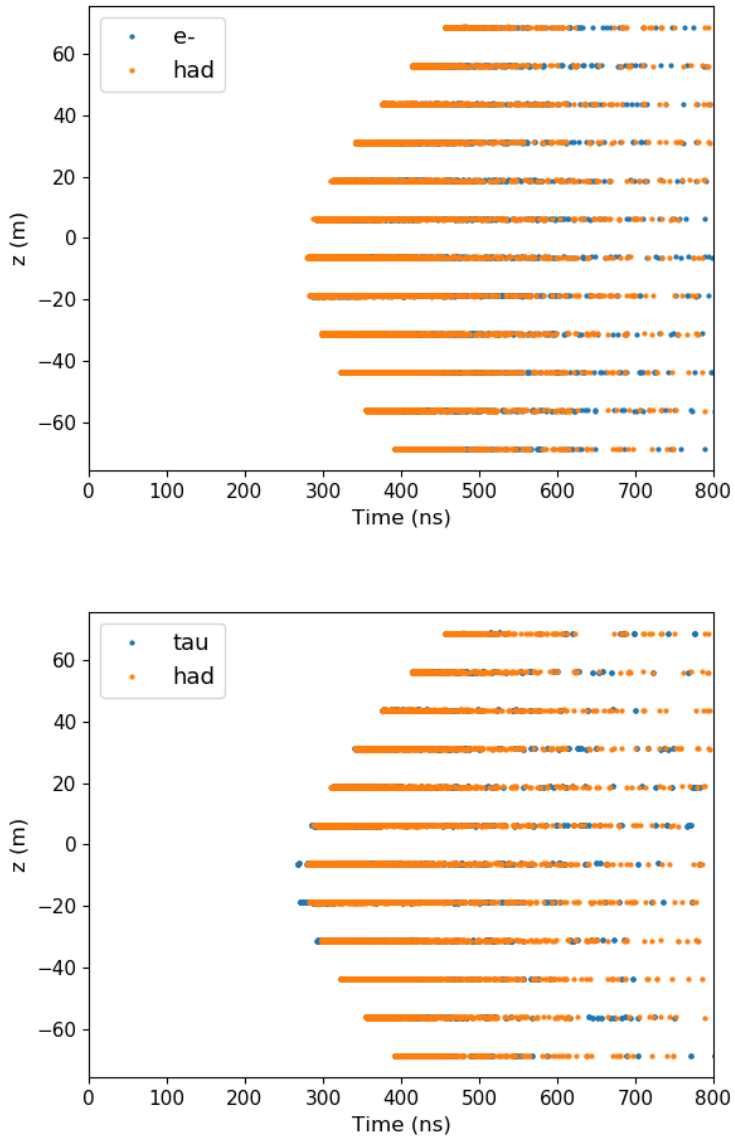

Figure 10: A plot of the time of the photon hits at different depths. Top: Plot for an e-neutrino event with an energy of 120 TeV. Bottom: Plot for a tau neutrino event with an energy of 120 TeV.

5.2 Time Residuals

The arrival time of the photons was binned with a minimum bin size of 1 ns for every sensor in every event. The time residual plot for 200 TeV tau and electron neutrino event is presented in Figure 11. Note the clear double peak signature for the tau neutrino event.

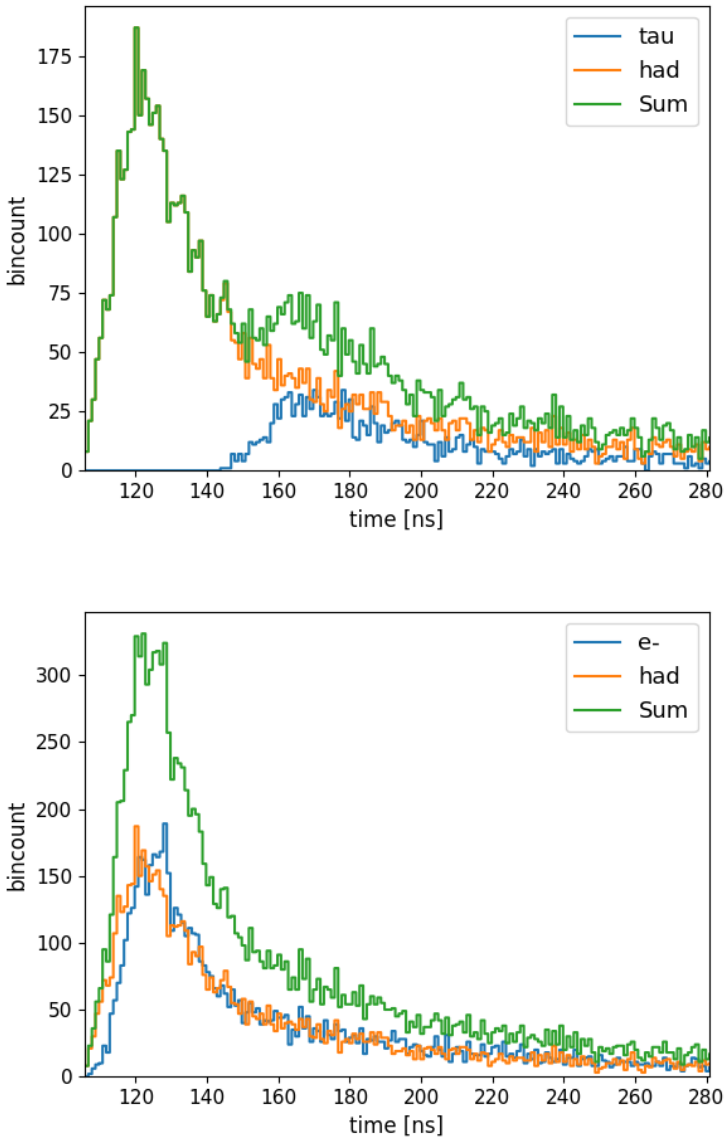

Figure 11: A plot of the distribution of photon arrival time from the GEANT4 simulation with the bin size fixed at 1 ns for a single PMT. Top: Tau neutrino simulation with a combined lepton and hadronic shower energy of 200 TeV. The tau decay time was 22.2 ns. Bottom: e-neutrino simulation with a combined lepton and hadronic shower energy of 200 TeV.

5.3 Time Residuals at Cerenkov Angle

Sensors near the Cerenkov angle ($\theta = 41.4°$) receive significantly more light as shown in Figure 12. Additionally, the timing difference between the hadronic shower and tau decay shower are negligible. Generally, it will be impossible to identify the a double peak pattern from sensors in this range. For our analysis We will not consider tau events that decay into muons.

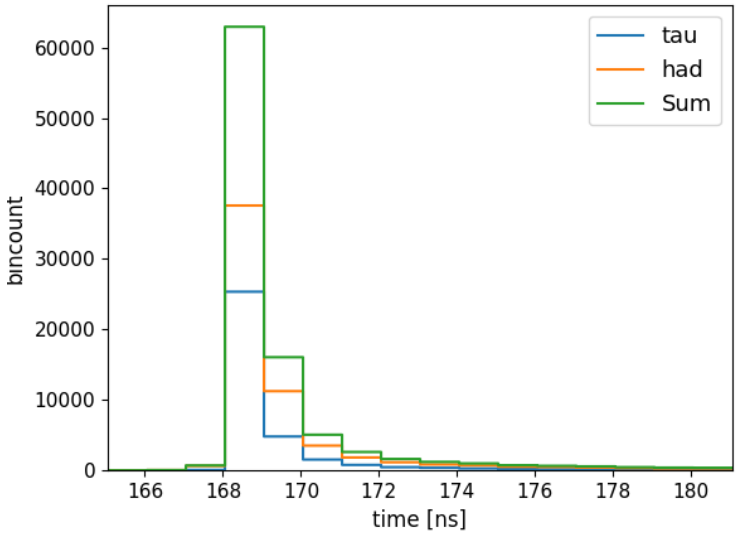

Figure 12: A plot time residuals with a 1 ns bin size for a single PMT close to the Cerenkov angle relative to the event vertex. The decay time for this event was 8.2 ns.

6 Curve Fitting Time Residuals

6.1 Fitting Function

The distribution of the photon arrival time from a lepton decay or hadronic shower, as seen in Figure 11, roughly resembles a gaussian. A better approximation would be a bifurcated gaussian, a gaussian with a different variance to the left and right. A sum of two gaussians or bifurcated gaussians will be needed to fit the double peak signal of tau neutrinos.

A comparison of a gaussian and bifurcated gaussianfit for a electron neutrino event at 100 TeV is presented in Figure 13. We see that the bifurcated gaussianproduces fits match the time residuals significantly better than a normal gaussian. Thus for our analysis, only bifurcated gaussianfits will be used.

For our analysis we included all the events at 50 and 100 TeV, except for the tau events that decayed into muons since those produce very little light. For each event, we analyzed the time residuals in the sensors in the 4 strings closest to the event vertex, excluding sensors close to the Cerenkov angle, and sensors farther than 80 m from the event vertex. For each sensor, we fitted the time residual with a single and double bifurcated gaussianwithin a time

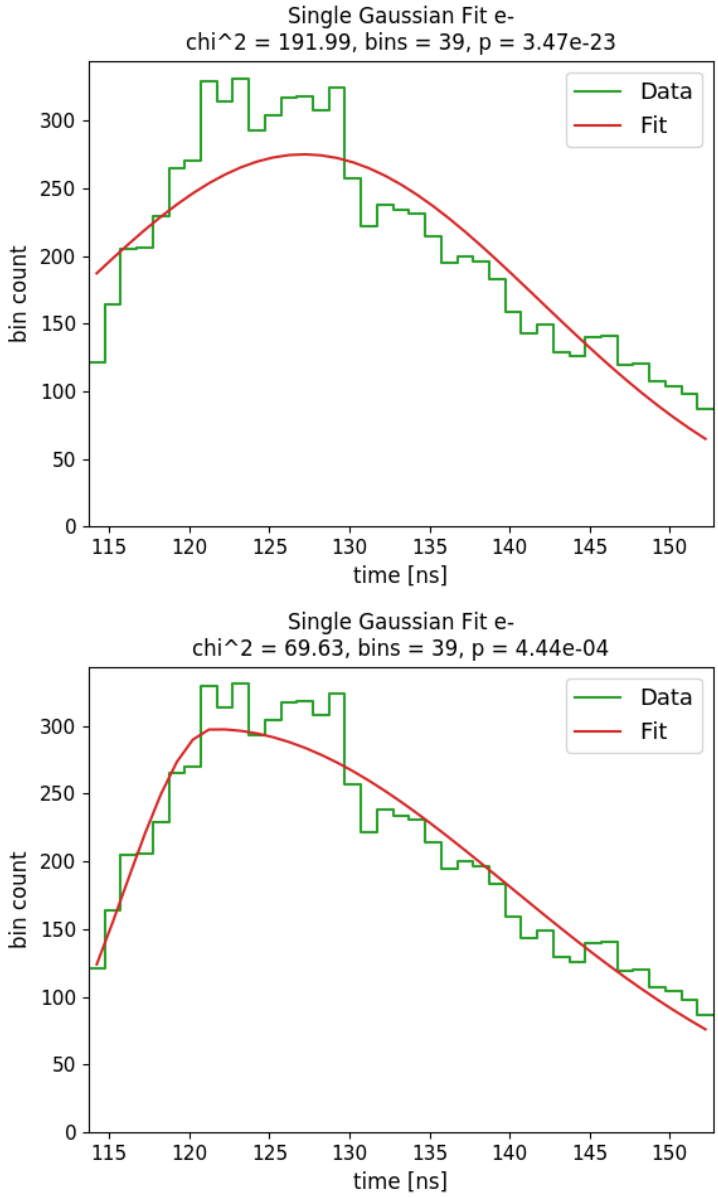

Figure 13: Curve fit of the time residuals for a 200 TeV electron neutrino event using a single gaussian (Top) and a single bifurcated gaussian (Bottom).

range corresponding to the full width at 1/4 or 1/3 the maximum value. This was done as a way to select an appropriate time range that excludes the tails of the time residuals, which could affect the curve fit. For each fit, the best fit parameters along with the χ^2 and p-value are returned. A sample fit of a 200 TeV tau neutrino event is presented in Figure 14

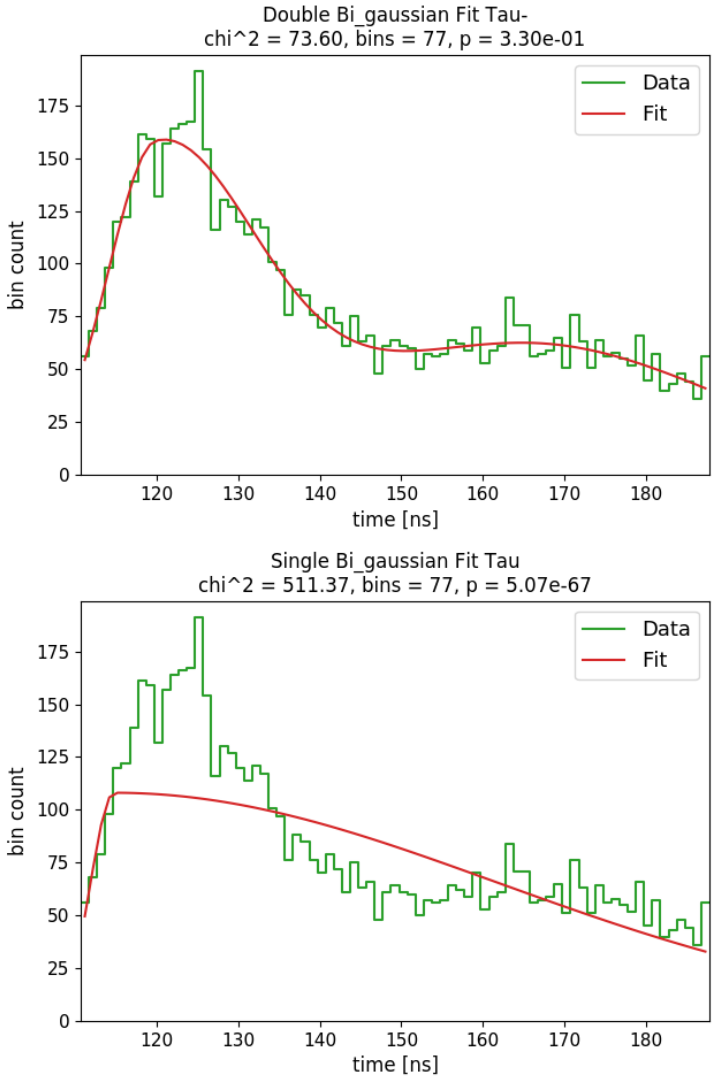

Figure 14: Curve fit of the time residuals for a 200 TeV tau neutrino event using a double bifurcated gaussian (Top) and a single bifurcated gaussian (Bottom).

7 Analysis

The aim of curve fitting tau and electron neutrino events is to identify tau events with a certain level of accuracy by studying the curve fitting parameters returned by the two fitting functions. The idea is that there would be a separation in the distribution of these parameters between electron and neutrino events. This method differs from the approach taken in [1], which explored tau identification by identifying a double peak in the time residuals.

7.1 Filtering the Fits

In order to obtain accurate results, bifurcated gaussianfits were filtered through to remove ones with terrible fitting parameters such as the one shown in Figure 15. This does not necessarily mean that the fit does not match the simulation data.

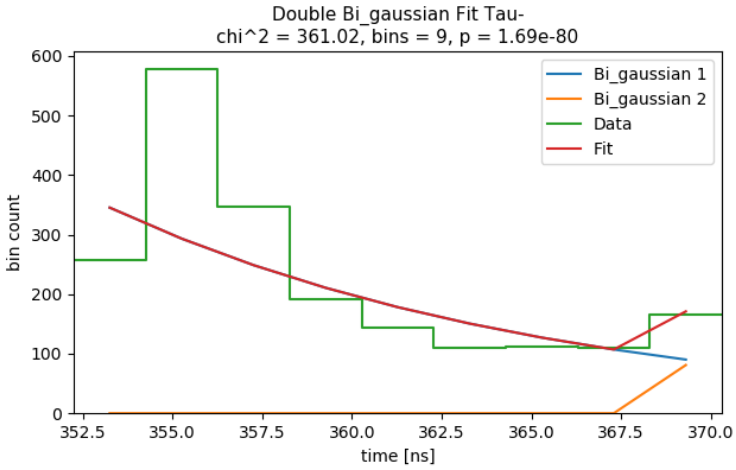

Figure 15: Example plot of a poor fit to the time residual.

To remove these fits, the time difference, amplitude ratio and FWHM ratio between the two gaussians in the double bifurcated gaussianfit were considered. Only fits with a time difference less than 100 ns and an amplitude and FWHM ratio between 1/4 and 4 were kept.

7.2 Fitting Results Analysis

Of all the distribution of the fitting results, the distribution of the time difference and p-value ratio show the most separation between tau and electron neutrino events. A plot of the two distributions is shown in Figure 16. The p-value and χ^2 ratio is the ratio between that parameter for the double bifurcated gaussianfit and the single bifurcated gaussianfit. Other parameters such the individual χ^2 value and p-value show slight separation, while others such as the amplitude ratio and FWHM ratio have no separation.

Further improvements filtering method could significantly improve the result. For instance, in the time difference plot in Figure 16, we see that some fits for the electron events returned a time difference between 60-100 ns. Additionally, a method of selecting the best sensor for each event, could also significantly improve the differentiation between electron and tau events.

7.3 ROC Curve Analysis

A receiver operator characteristic (ROC) curve, was plotted for the three fitting parameters explored; the time difference, p-value ratio and χ^2 ratio. A plot of the ROC curve for 100 TeV and 50 TeV are shown in Figure 17. A ROC curve plots the true positive rate (TPR) against the false positive rate (FPR) and the area under curve (AUC) is the accuracy of the classification. For instance, a AUC of 1 is a perfectly accurate identification, while a AUC of

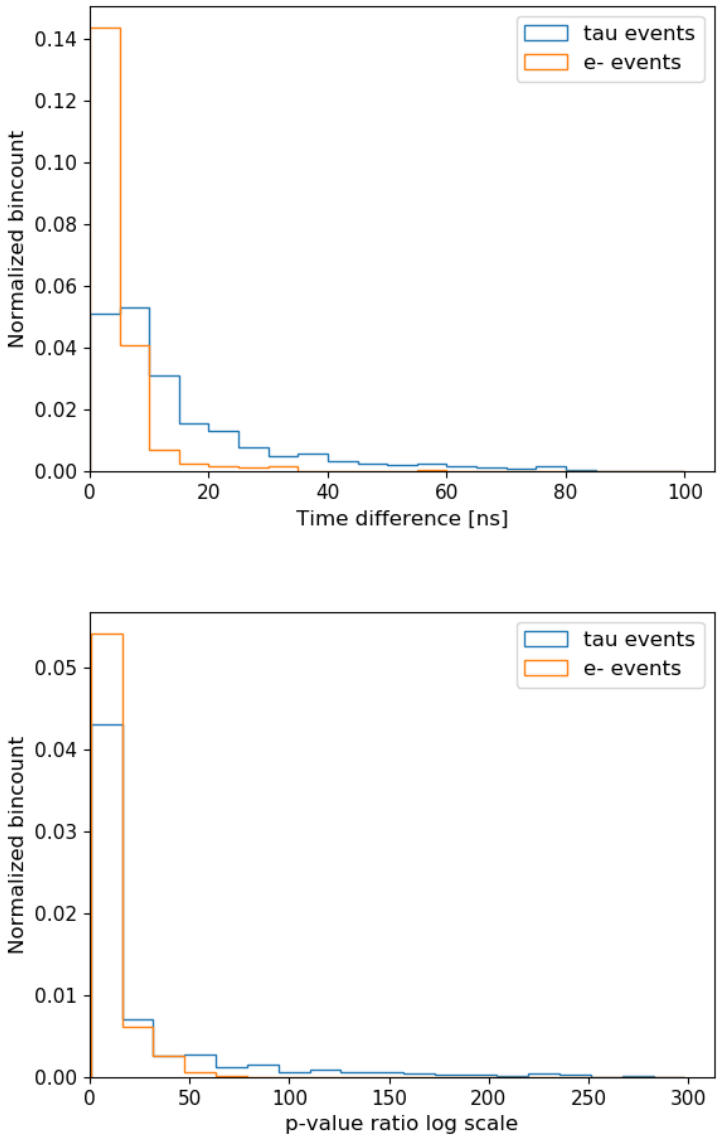

Figure 16: Plot of the distribution of time difference (top) and the p-value ratio (bottom) for e- events and tau events.

0.5 indicates the classification is completely random. We see inf 17 that the AUC is better for the 100 TeV compared to the 50 TeV.

This analysis provides a rough idea for the detection identification accuracy at a specific energy. Beyond looking separation in 1 dimension, better differentiation may be achieved by including more parameters in various ways. For example, Figure 18, shows a scatterplot in the two dimensions that showed the most separation. We see that better separation between

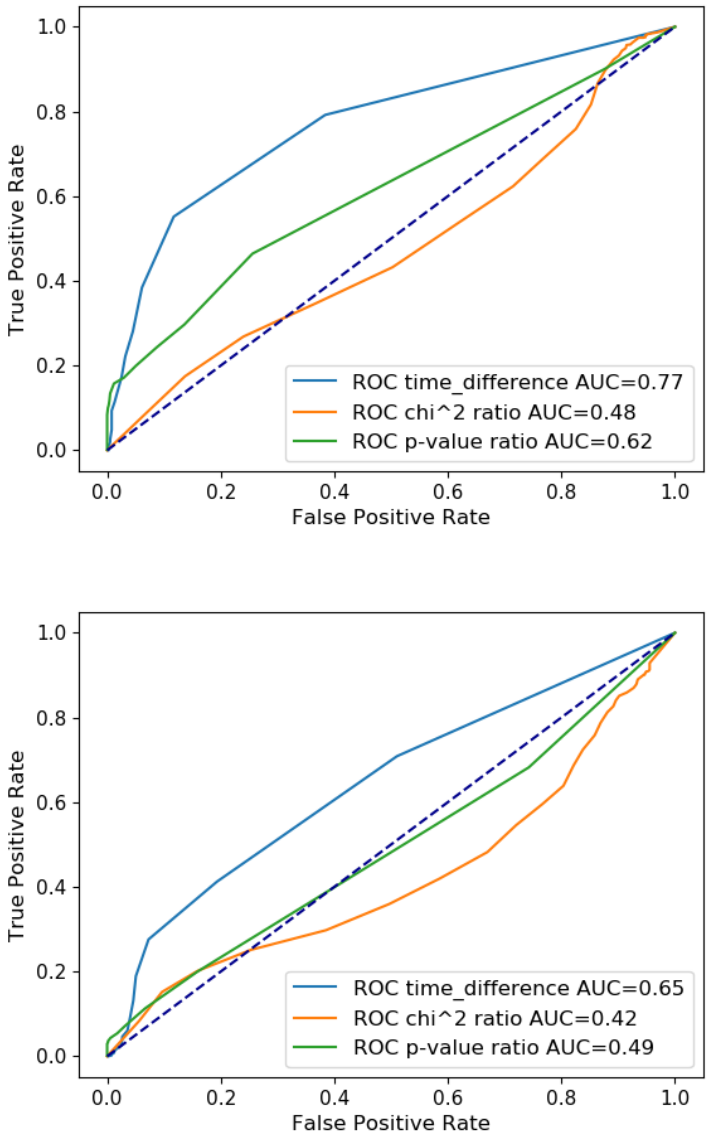

Figure 17: ROC curve analysis for all the events at 100 TeV (top) and 50 TeV (bottom).!!!

tau and electron neutrino events could be achieved by binning along a diagonal line.

7.4 Bin by Decay Time and Hits

Another method of classifying the events are by decay times and the number of hits. This could provide a better idea of the identification accuracy instead of simply analyzing by energy. The ROC curve at these different bins for the time difference are summarized in

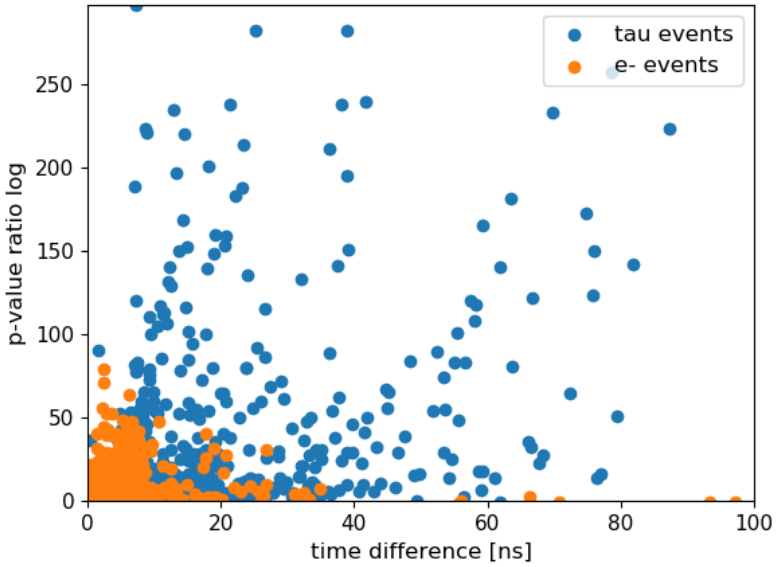

Figure 18: Plot of the time difference and p-value ratio for all the 100 TeV events.

Table 4 and 5.

Energy (TeV)	Decay Time Range	Hits Range	AUC
100	All	All	0.72
100	30 - 60 ns	200 000 - 360 000	0.95
100	30 - 60 ns	40 000 - 200 000	0.92
100	15 - 30 ns	200 000 - 360 000	0.85
100	15 - 30 ns	40 000 - 200 000	0.87
100	7 - 15 ns	200 000 - 360 000	0.75
100	7 - 15 ns	40 000 - 200 000	0.80
100	0 - 7 ns	200 000 - 360 000	0.62
100	0 - 7 ns	40 000 - 200 000	0.57

Table 4: The AUC for the ROC curve of the time difference at different decay time range and hits range for the 100 TeV events.

Generally, we see that the difference between the number of hits has little effect on the AUC. Further more, the same decay time range at the two different energies have comparable values for the AUC. Assuming a 90% accuracy in detecting tau neutrino events with a decay time greater than 30 ns and 80% in detecting events with a decay time greater than 15 ns, regardless of energy and the number of photon hits, we can estimate the percentage of events that can be detected based on the probability of a tau decay time with a range greater than 30 ns or 15 ns at a specific energy. Figure 19 is a plot of this detection rate as a function of energy.

Energy (TeV)	Decay Time Range	Hits Range	AUC
100	All	All	0.64
50	15 - 30 ns	100 000 - 180 000	0.82
50	15 - 30 ns	20 000 - 100 000	0.80
50	7 - 15 ns	100 000 - 180 000	0.71
50	7 - 15 ns	20 000 - 100 000	0.65
50	0 - 7 ns	100 000 - 180 000	0.55
50	0 - 7 ns	20 000 - 100 000	0.59

Table 5: The AUC for the ROC curve of the time difference at different decay time range and hits range for the 50 TeV events.

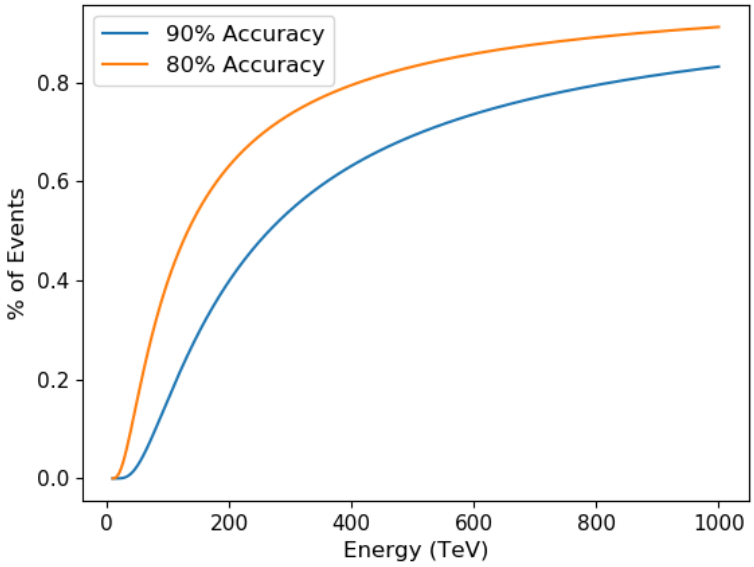

Figure 19: Plot of the detection rate at various energies.

The analysis here should simply be treated as preliminary, since only a total of 100 events were produced, each bin only contained roughly 10 events. Many more events will need to be simulated to give a better idea of the statistics, and provide a better estimate of the detection accuracy.

8 Summary/Next Steps

For this project 100 tau neutrino and e- neutrino events were simulated at 200 TeV, 100 TeV, 20 TeV with the energy split evenly between the lepton and the hadronic shower. The arrival time of the photons for each sensor was binned and plotted. Several sensors were chosen and for each event at 200 TeV and 100 TeV, all the time residuals were fitted with a single bifurcated gaussianand double bifurcated gaussianreturning the fitting parameters,

χ^2 and p-value. By analyzing the different parameters returned, we see a separation in the time difference, p-value ratio between tau neutrinos and e- neutrinos events. A ROC curve analysis was done, giving a measure of how well we can differentiate between the two types of events using different parameters. Additionally, by giving a rough detection accuracy for a given decay time range regardless of the energy, we obtain a plot of the detection rate as a function of energy.

Overall, this project gives a preliminary study into the detection accuracy for tau neutrinos at different energies or decay time range. Thus this could be used to calculate the flux of tau neutrinos that could be detected by the future P-ONE detector and generally give a sense of the limit of tau neutrino identification.

To improve this study and increase the statistics many more events should be simulated. More energies should be explored but also different combination of lepton and hadronic shower energy to better understand the effect the relative amount of light produced by the hadronic shower and lepton has on the fits. Better methods that can select the best fits for each event would greatly improve the detection accuracy, and also an analysis with more variables such as a scatterplot could lead to better differentiation between tau and e- neutrinos.

References

[1] Xiao, Meng. "The Limit of Tau Neutrino Detection" (2019)

[2] Man, Matthew. "Optical Properties of Seawater at P-ONE Site" (2019)

[3] Henningsen, Felix. "STRAW (STRings for Absorption length in Water): pathfinder for a neutrino telescope in the deep Pacific Ocean." EPJ Web Conf.. Vol. 207. 2019.

[4] http://pdg.lbl.gov/2019/reviews/rpp2018-rev-tau-branching-fractions.pdf